Carbohydrate Polymers 100 (2014) 158–165

Contents lists available at ScienceDirect

Carbohydrate Polymers

journal homepage: www.elsevier.com/locate/carbpol

An effect of alginate on the stability of LDH nanosheets in aqueous solution and preparation of alginate/LDH nanocomposites

Hongliang Kang[a], Yang Shu[a,b], Zhuang Li[a], Bo Guan[c], Shunjin Peng[b], Yong Huang[a,*], Ruigang Liu[a,*]

[a] State Key Laboratory of Polymer Physics and Chemistry, Beijing National Laboratory of Molecular Sciences, Institute of Chemistry, Chinese Academy of Sciences, Beijing 100190, China
[b] School of Materials and Metallurgy, Wuhan University of Science and Technology, Wuhan 430081, China
[c] Center for Physicochemical Analysis and Measurement, Institute of Chemistry, Chinese Academy of Sciences, Beijing 100190, China

ARTICLE INFO

Article history:
Received 3 August 2012
Received in revised form 21 July 2013
Accepted 22 July 2013
Available online 25 July 2013

Keywords:
Alginate
Layered double hydroxide (LDH)
Dispersion
Stabilization
Nanocomposite

ABSTRACT

Nanosheets under 10 nm in thickness are obtained by exfoliating layered double hydroxide (LDH) in formamide. The LDH nanosheets are dispersed and stabilized in an alginate aqueous solution after removing formamide by water washing and ultracentrifugation. During the water washing stage LDH nanosheets can be prevented from restacking by electrostatic stabilization of the surface of LDH sheets through the adsorption of alginate. Alginate/LDH nanocomposites can be prepared by drying the dispersion, and sandwich-like structures in the nanocomposites are formed with two alginate layers contained between two LDH sheets. LDH nanosheets in the dried alginate/LDH nanocomposites can be re-dispersed in water. The thermal stability of alginate in the nanocomposite is increased by LDH. Alginate membranes containing this layered nanocomposite can be prepared. The addition of LDH into the alginate matrix leads to an increase in the mechanical properties of the nanocomposite.

1. Introduction

Two-dimensional (2D) nanomaterials such as nanosheets or nanoplates have attracted increasing interests in recent years due to their potential applications in the fields of gas storage and separation, catalysts, sensors, support membranes and inert coatings (Mas-Balleste, Gomez-Navarro, Gomez-Herrero, & Zamora, 2011). The origins of 2D nanomaterials include layered hydroxides (Hibino, 2004), smectite clays (Lee & Kim, 2002; Sasaki & Watanabe, 1998), graphite oxides (Knieke et al., 2010; Kuila et al., 2011; Nethravathi & Rajamathi, 2008; Widenkvist et al., 2009), dichalcogenides (Ayari, Cobas, Ogundadegbe, & Fuhrer, 2007; Gordon, Yang, Crozier, Jiang, & Frindt, 2002; Li, 2010), metal phosphates (Takei, Yonesaki, Kumada, & Kinomura, 2008), and layered oxides (Masuda, Hamada, Seo, & Koumoto, 2006; Osada & Sasaki, 2009; Xiao, Chen, Ji, Zhang, & Yang, 2007). Layered double hydroxides (LDHs) are composed of a kind of positively charged brucite-type layered inorganic material with the general formula of $M^{II}_{1-x}M^{III}_{x}(OH)_2(A^{n-})_{x/n}\cdot mH_2O$, where M^{II} and M^{III} are respectively divalent and trivalent cations and A^{n-} is a n-valent anion. They consist of a stack of positively charged metal hydroxide layers with counter anions and water molecules in the interlayers. LDHs could be used in a wide range of applications including catalyst supports (Ma, Chai, Evans, Li, & Feng, 2011; Parvulescu et al., 2011), anion exchange units (Manohara, Prasanna, & Kamath, 2011), and fire retardant additives (Jiao, Chen, & Zhang, 2010; Wang et al., 2010).

Nanosheets are generally nanometer scale in thickness and micrometer scale in width, and can be obtained by delaminating the layered inorganic solids into single or multi-layered sheets. The properties of the nanosheets, such as optical and electronic properties, are quite different from the original layered materials due to the differences in the confined states of the electrons and the absence of interlayer interactions (Ida, Ogata et al., 2008; Novoselov et al., 2004; Osada, Ebina, Takada, & Sasaki, 2006). The geometric effect and the high specific surface area impart to the nanosheets specific mechanical and chemical properties (Rabu & Drillon, 2003; Ray & Okamoto, 2003).

Efforts toward the preparation of single layered nanosheets in solutions have been reported. Micromechanical exfoliation in solution has been reported as an effective preparation of graphite (Sakamoto, van Heijst, Lukin, & Schluter, 2009), BN, MoS_2, $NbSe_2$ and $Bi_2Sr_2CaCu_2O_x$ (Novoselov et al., 2005) nanosheets. But the thickness of nanosheets prepared by micromechanical exfoliation is generally large, which limits their applications. An alternative method has been developed to delaminate solids and form

* Corresponding authors. Tel.: +86 10 82618573; fax: +86 10 82618573.
E-mail addresses: yhuang@iccas.ac.cn (Y. Huang), rgliu@iccas.ac.cn (R. Liu).

0144-8617/$ – see front matter © 2013 Elsevier Ltd. All rights reserved.
http://dx.doi.org/10.1016/j.carbpol.2013.07.051

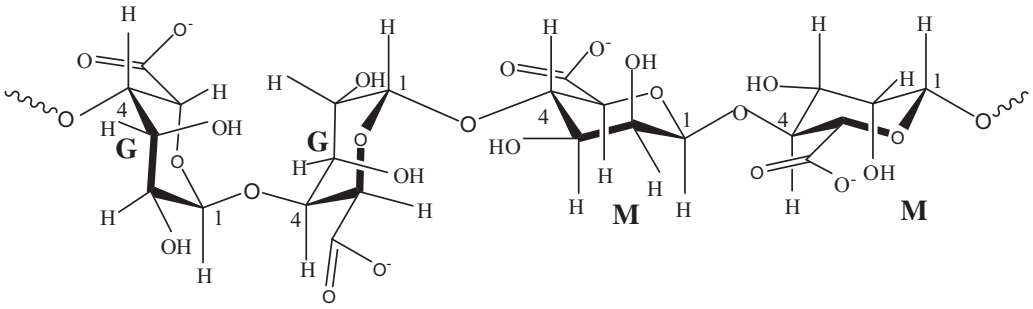

Scheme 1. Structure of alginate.

colloidal solutions of single-layered nanosheets; this method is based on chemical modification of the layers to increase the interlayer repulsive forces. Typical examples include the exfoliation of the manganese (Omomo, Sasaki, Wang, & Watanabe, 2003), cobalt (Kim et al., 2009), and titanium oxides (Tanaka, Ebina, Takada, Kurashima, & Sasaki, 2003) into colloidal solutions after protonation and the exfoliation of a nickel layered hydroxide in formamide by intercalation with dodecyl sulfate ions (Ida, Shiga, Koinuma, & Matsumoto, 2008). Much research into the delamination of LDHs into nanosheets (Adachi-Pagano, Forano, & Besse, 2000; Hibino & Jones, 2001; Hibino & Kobayashi, 2005; Li, Ma, Ebina, Iyi, & Sasaki, 2005; Liu et al., 2006) has been carried out and it was found that formamide was an excellent delaminating agent for highly crystalline LDHs after intercalation with NO_3^- groups in the interlayers (Hibino & Jones, 2001; Li et al., 2005; Liu et al., 2006). However, the exfoliated nanosheets are unstable and will reassemble into thick layered structures after removing the delamination media. Stabilization of the exfoliated nanosheets is one of the key points necessary for further development of applications. Stabilization of the exfoliated nanosheets has been tried, *e.g.* the stabilization of graphene oxide sheets by covalently bonded amine-modified polyethylene glycol dendrimers (Liu, Robinson, Sun, & Dai, 2008) or by the steric stabilizer Pluronic F127 (Hong, Compton, An, Eryazici, & Nguyen, 2012). In the case of LDHs with a positively charged surface of each layer, polymers with functional groups that can interact with the nanosheets could be used as the stabilizers of the LDH nanosheets. In previous works, carboxymethyl cellulose (CMC) has been successfully used for the stabilization of LDH nanosheets. The LDH nanosheets can be stabilized in their colloidal state even after replacing the delamination media formamide with water (Kang et al., 2009). Also, LDH nanosheets stabilized with CMC will restack into a layered structure after evaporating water.

Alginate is an anionic polysaccharide and consists of β-D-mannuronate (M) and α-L-guluronate (G) units with different M/G ratios depending on origin (Scheme 1). The abundant hydroxyl and carboxyl groups along alginate chains could lead to strong interactions with the positively charged surface of LDH nanosheets. Alginate/LDH composites have been prepared by the incorporation of alginate chains into the interlayers of LDHs *via* direct coprecipitation (Darder, Lopez-Blanco, Aranda, Leroux, & Ruiz-Hitzky, 2005; Leroux, Gachon, & Besse, 2004). Mesoporous alginate/LDH composite beads, with high specific surface area and high activity, have the potential for controlled drug release applications (Alcantara, Aranda, Darder, & Ruiz-Hitzky, 2010; Zhang, Wang, Xie, Li, & Wang, 2010). However, the interactions between the alginate molecules and LDH, as well as the stabilization of LDH with alginate, have been somewhat overlooked in the literature.

In this paper, stabilization of LDH nanosheets by alginate in aqueous media and distribution of the LDH nanosheets in the alginate/LDH nanocomposites were investigated. Thermal stability and mechanical properties of alginate/LDH nanocomposites were also investigated. It was found that the LDH nanosheets can be stabilized by alginate molecules in aqueous media and the LDH nanosheets in the nanocomposites can be re-dispersed in aqueous media.

2. Experimental

2.1. Materials

Sodium alginate (Acros, from brown algae, viscosity of ~250 cps of 2 wt.% solution at 25 °C) with M/G ratio about 1.09 (estimated by the intensity of IR absorption bands of —OH and C—O—C on the FTIR spectrum (Sakugawa, Ikeda, Takemura, & Ono, 2004)) was used as received. All other chemicals (AR grade) were supplied by local chemical suppliers and used as received.

2.2. Synthesis of the NO_3^-–LDH and exfoliation

Highly crystallized MgAl–CO_3^{2-} LDH was synthesized through a hydrothermal process (Ogawa & Kaiho, 2002). A mixed solution containing $Mg(NO_3)_2$ (0.1 mol/L), $Al(NO_3)_3$ (0.05 mol/L) and urea (0.5 mol/L) was hydrothermally treated at 100 °C for 34 h in a Teflon-autoclave. The precipitate was filtered, washed, and then dried at 30 °C in vacuum resulting in the CO_3^{2-}–LDH. The CO_3^{2-} groups in the CO_3^{2-}–LDH were replaced with NO_3^- groups by treating the CO_3^{2-}–LDH with HNO_3–$NaNO_3$ aqueous solution (Iyi, Okamoto, Kaneko, & Matsumoto, 2005) to result in NO_3^-–LDH. The delamination of NO_3^-–LDH was achieved in formamide. Typically, 0.15 g of NO_3^-–LDH was dispersed in 150 mL of formamide. The mixture was sealed after purging with nitrogen, and then vigorously stirred for 24 h to result in a colloidal solution, in which the LDH was exfoliated into nanosheets.

2.3. Stabilization of LDH nanosheets with alginate and preparation alginate/LDH nanocomposites

An aqueous solution of alginate (6.7 g/L) was added dropwise into a LDH colloidal solution (1.0 g/L) with continuous stirring and purging with nitrogen. The mixture of the two solutions comprising of the alginate aqueous solution and the LDH colloidal solution gave the volume ratios of 0.8:1 and 0.6:1 (corresponding to the alginate/LDH weight ratios of 8.6:1 and 6.5:1, respectively). The mixed solution was then centrifuged at 10,000 rpm. The supernatant liquid was removed and the lower colloidal layer was washed several times with degassed water, resulting in a colloidal mixture.

Alginate/LDH nanocomposites were prepared by evaporating the water of the resultant colloidal mixture through freeze-drying or by drying at 40 °C *in vacuo*. The alginate content in the resultant composites was about 37% (estimated by carbon content) and was independent of the initial ratio of alginate to LDH.

Alginate/LDH nanocomposite films were prepared by mixing solutions of the alginate aqueous solution (6.7 g/L) and the LDH

Table 1
Results of chemical analysis of LDH and alginate/LDH nanocomposites.

Samples	Content, Found (Calcd)/wt.%						Formula
	Mg	Al	C	H	N	Na	
CO_3^{2-}–LDH	16.46 (16.68)	12.77 (12.94)	2.86 (2.90)	4.07 (4.13)	–	–	$Mg_{0.59}Al_{0.41}(OH)_2(CO_3)_{0.21}\cdot 0.76H_2O$
NO_3^-–LDH	16.10 (15.65)	11.73 (11.40)	0.88 (0.85)	3.50 (3.38)	5.07 (4.93)	–	$Mg_{0.62}Al_{0.41}(OH)_2(NO_3)_{0.34}(CO_3)_{0.07}\cdot 0.64H_2O$
Alginate/LDH nanocomposite-I[a]	7.42 (7.82)	10.16 (10.71)	14.50 (15.24)	4.68 (4.93)	0.06 (0.11)	0.11 (0.11)	$Mg_{0.40}Al_{0.49}(OH)_2(C_6H_7O_6)_{0.26}\cdot 1.11H_2O\ (NaNO_3)_{0.006}$
Alginate/LDH nanocomposite-II[b]	8.49 (9.29)	10.31 (11.28)	14.21 (15.54)	4.06 (4.44)	0.11 (0.13)	0.22 (0.23)	$Mg_{0.43}Al_{0.46}(OH)_2(C_6H_7O_6)_{0.24}\cdot 0.62H_2O\ (NaNO_3)_{0.011}$

[a] The volume ratio of alginate aqueous solution and LDH formamide solution is 0.8/1.
[b] The volume ratio of alginate aqueous solution and LDH formamide solution is 0.6/1.

colloidal solution (1.0 g/L), at the volume ratios of 0.8:1 and 0.6:1, and directly dialyzing against water to remove the formamide. The resulting solutions had weight ratios of alginate and LDH of 8.6:1 and 6.5:1, respectively. The solutions were then poured into a circular Teflon mold and vacuum dried at 40 °C to generate alginate/LDH nanocomposite films.

2.4. Characterizations

The carbon, hydrogen and nitrogen contents of the MgAl–NO_3^- LDH and alginate/LDH nanocomposites were determined by the CHN analysis and the magnesium and aluminum contents were determined by inductively coupled plasma (ICP) atomic emission spectroscopy (Varian 710-ES, USA) after nitric acid decomposition. FT-IR transmittance spectra were recorded on a Bruker-Equinox 55 FT-IR spectrometer at room temperature. Powder X-ray diffraction (XRD) patterns of the samples were collected using a Philips X'Pert diffractometer with Cu $K\alpha$ radiation. Powder discs of the LDHs and films of the alginate/LDH nanocomposites were used for the XRD measurements. The alginate/LDH nanocomposites were embedded in an epoxy resin then microtomed using a diamond knife to prepare sections for TEM observations. TEM observations were conducted on a JEM-2011. Thermogravimetry (TGA) (Pyris 1 TGA, Perkin Elmer) was carried out in the temperature range 20–700 °C in flowing N_2 at a heating rate of 10 °C/min. Stress–strain measurements were carried out on a universal material testing machine (INSTRON 5699, USA). Zeta potential and particle size measurements were carried out with a Brookhaven Zetaplus analyzer (Brookhaven Instruments Corp.) Atom force microscopy (AFM) images were collected with a Multimode 8 scanning probe microscopy (BRUKE Vecoo) in the tapping mode. Silicon tips on cantilevers (resonance frequency 300 kHz) with a spring constant of 32 N m^{-1} were used. The scanning rate was in the range 0.5–1.0 Hz. Samples for AFM measurements were prepared by spin-coating 10 μL of the solution onto a freshly cleaved mica surface and evaporating the solvent at room temperature.

3. Results and discussion

3.1. LDH nanosheets

The MgAl–CO_3^{2-} LDH crystals synthesized in the present work are of uniform hexagonal shape with an average lateral size of 1.5 μm, thickness of 0.3 μm (Fig. 1A) and composition of $Mg_{0.59}Al_{0.41}(OH)_2(CO_3)_{0.21}\cdot 0.76H_2O$ (Table 1). After the CO_3^{2-} groups are replaced with NO_3^- groups the basal spacing of the resultant MgAl–NO_3^- LDH is 0.89 nm, changing from 0.76 nm in the carbonate form (Fig. 1C). The MgAl–NO_3^- LDH crystals retain hexagonal symmetry with lattice parameters of a = 3.0362 nm and c = 26.714 nm and composition of $Mg_{0.62}Al_{0.41}(OH)_2(NO_3)_{0.34}(CO_3)_{0.07}\cdot 0.64H_2O$ (Fig. 1B and Table 1). The absorption bands at 1353 cm^{-1} (Fig. 1D-a) and 1384 cm^{-1} (Fig. 1D-b) on the FTIR spectra confirm the presence of CO_3^{2-} and NO_3^-, respectively. The NO_3^-–LDH was treated in formamide at a concentration of 1 g/L at room temperature resulting in exfoliated 2-dimensional nanosheets.

The Tyndall effect of the exfoliated nanosheets of MgAl–NO_3^{2-} LDH can be seen (Fig. 2A'), the average particle size of the LDH nanosheets in formamide is 507 nm and the size distribution is shown in Fig. 2A. The TEM image of the exfoliated nanosheets of MgAl–NO_3^{2-} LDH (Fig. 2B) shows irregular micron-sized thin plates, indicating that LDH nanosheets are cracked after exfoliating in formamide. The AFM image (Fig. 2C) also shows irregular shape sheets under 10 nm in thickness. Colloidal LDH nanosheets were obtained through centrifugation and removal of the supernatant liquid. Fig. 2D-a shows the powder XRD pattern of colloidal LDH nanosheets. A halo and a small peak (2θ = 61°, d = 0.15 nm) of the (110) plane of LDH layer can be observed. These results indicate that the crystalline LDH is exfoliated to nanosheets in formamide.

3.2. Stabilization of LDH nanosheets by alginate in aqueous solution

The LDH nanosheets are sensitive to water and they will restack into a lamellar form immediately (Kang et al., 2009). In this work, an alginate aqueous solution was added to a colloidal suspension of LDH nanosheets in formamide, keeping the volume of formamide greater than that of the aqueous solution. No precipitation was observed in the resultant mixed solutions and Tyndall light scattering phenomenon could be observed suggesting that the exfoliated LDH nanosheets did not restack during the addition of alginate aqueous solution.

The mixture was concentrated by centrifugation to form a transparent colloidal substance which separated from the formamide/water solution. Powder XRD results of resultant alginate/LDH colloidal mixture indicated that it had a similar diffraction pattern (Fig. 2D-b) to that of the colloid of LDH (Fig. 2D-a), indicating that neither the alginate nor the water had an effect on the colloidal state of LDH nanosheets. The mixed solution was then washed with large volumes of water and centrifuged. A typical XRD curve of the washed mixed colloidal solution showed that there were no new diffraction peaks (Fig. 2D-c) compared with the unwashed mixed colloid solution (Fig. 2D-b), with only a halo and a small peak (2θ = 61°, d = 0.15 nm) of the (1 1 0) plane of LDH layer, suggesting that the nanosheets had not restacked. The halo of the washed sample had shifted to a higher 2θ than that of the unwashed sample (Fig. 2D-b), in the 2θ range 20–55°, which is due to the removal of formamide. The characteristic FTIR absorption bands of formamide at 1690 and 1311 cm^{-1} (Fig. 3a) disappear from the FTIR spectra after the mixture is washed with excess water (Fig. 3b), which confirms the removal of formamide. Moreover, the existence of the characteristic absorbance bands of alginate on the FTIR spectra is indicative of alginate absorption on the LDH nanosheets; for example, the 1411 and 1633 cm^{-1} bands for the

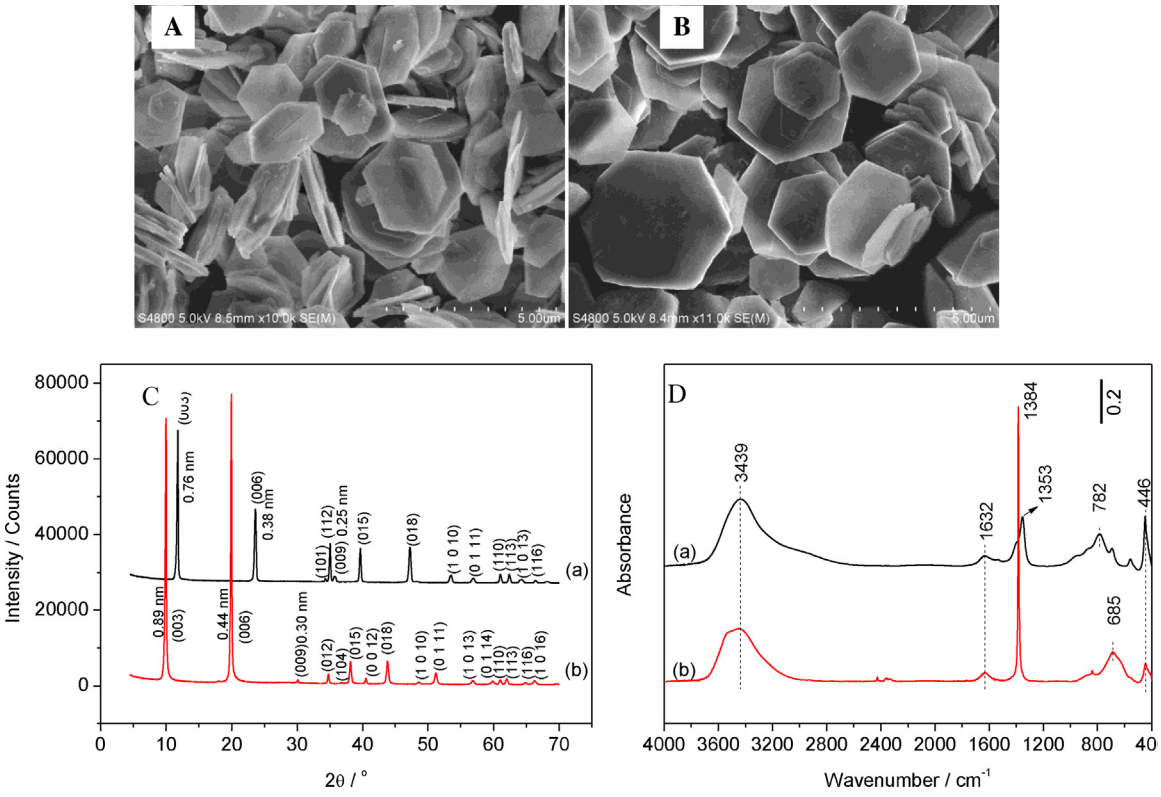

Fig. 1. SEM photos (A) and (B), XRD patterns (C) and FTIR spectra (D) of (a) CO_3^{2-}–LDH and (b) NO_3^-–LDH.

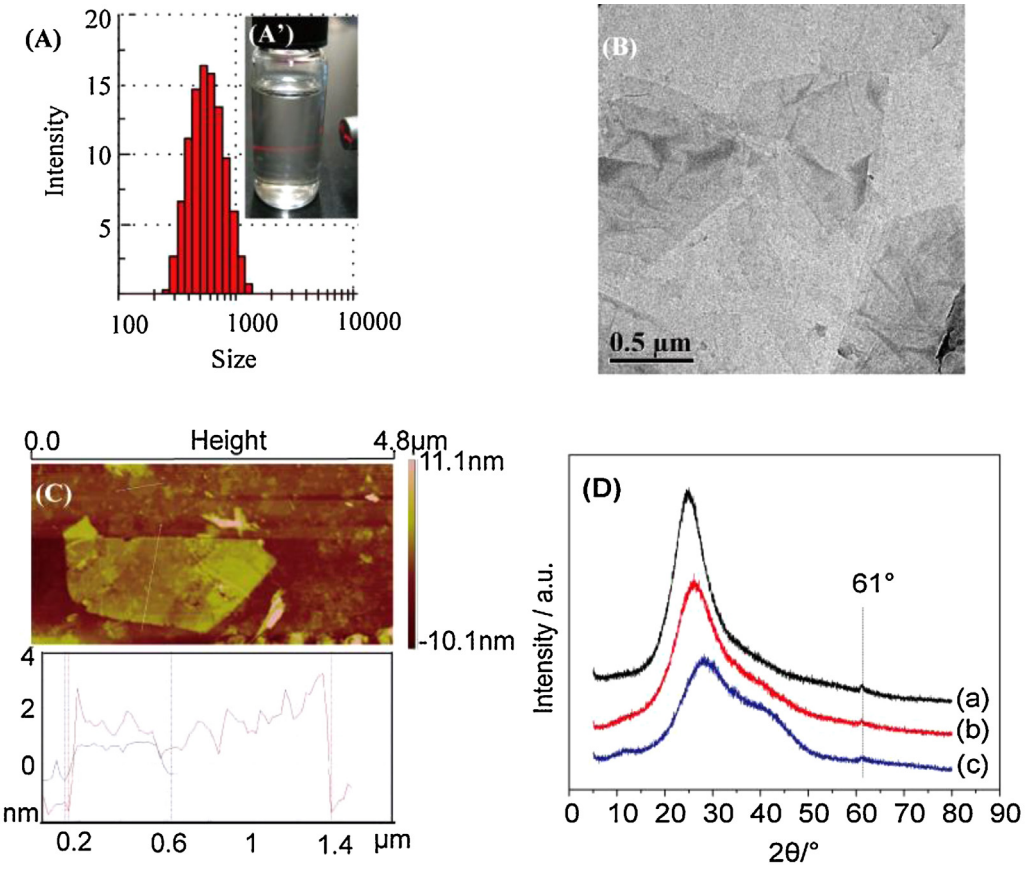

Fig. 2. Particle size distribution (A), Tyndall effect (A'), TEM (B) and AFM (C) photos of LDH nanosheets in formamide, and powder XRD patterns (D) of (a) colloid suspension of LDH nanosheets, (b) colloidal mixed suspension of alginate and LDH nanosheets with volume ratio of 0.8:1, (c) the sample after the mixed suspension (b) was washed with water.

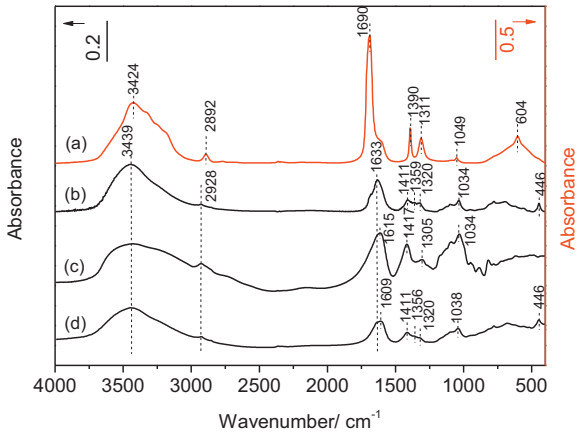

Fig. 3. FTIR spectra of (a) colloid suspension of alginate and LDH nanosheets (0.8:1, V/V), (b) the sample after the suspension (a) was washed with water, (c) alginate, (d) dried alginate/LDH nanocomposite.

symmetric stretching vibration of —COO^- and the stacking band of the typical antisymmetic vibration of —COO^- in alginate and the stretching vibration of H_2O molecule, respectively (Fig. 3b), suggest that alginate molecules are still adsorbed on the LDH nanosheets after water washing and centrifugation. The zeta potential of the alginate/LDH complex in an aqueous solution (0.112 mg/mL) (−32.2 mV) is higher than that of a pure alginate aqueous solution (0.154 mg/mL) (−76.2 mV), which indicates that there is an interaction between the alginate molecules and LDH nanosheets.

3.3. *Layered alginate/LDH nanocomposites by restacking of the LDH nanosheets adsorbed on alginate in the dried state*

Water washing and separation of the alginate/LDH mixture by ultracentrifugation removes the formamide as well as any alginate molecules that are not adsorbed on the surfaces of the LDH nanosheets. The LDH nanosheets with adsorbed alginate molecules, isolated by ultracentrifugation, were dried to obtain nanocomposites. The elemental contents in the dried alginate/LDH nanocomposites are listed in Table 1. Traces of Na and N elements in the nanocomposites are detected (Table 1), which are from the original materials of alginate and NO_3^-–LDH. The band at 1384 cm^{-1} in Fig. 3d and the basal spacing of 0.89 nm of the nitrate form in Fig. 4a–d all disappear, which suggests that a nitrate type phase does not exist in the alginate/LDH nanocomposites. The two alginate/LDH nanocomposites prepared resulted in the same alginate content, about 37 wt.% of alginate (estimated by carbon content), which was far less than the initial alginate ratio in the feedstock, and this alginate content was independent of the initial feedstock ratio of alginate to LDH. The results noted above suggest that only alginate molecules adsorbed on the LDH nanosheets were left after the water washing and centrifuging purification. The average area per unit charge (S_{charge}) of LDH nanosheets, calculated from the crystal parameter a of MgAl–NO_3^- LDH, is $3a^2 \sin 60^\circ = 0.239\ nm^2$/charge (Kang et al., 2009). Alginate macromolecules contain β-D-mannuronate (M) and α-L-guluronate (G) blocks. The diffraction signals of polymannuronic acid (M) and polyguluronic acid (G) were indexed on a two-chain orthorhombic unit cell with dimensions of $a = 0.76$ nm, $b = 0.86$ nm, $c = 1.04$ nm and $a = 0.86$ nm, $b = 1.07$ nm, $c = 0.87$ nm (chain direction), respectively (Fabia et al., 2005). We have estimated the values of S_{charge} for M and G respectively to be 0.327 and 0.460 nm^2/charge. The M/G ratio of alginate in this work is about 1.09 (Sakugawa et al., 2004), and the S_{charge} of alginate is about 0.391 nm^2/charge, which is larger than that of LDH nanosheets. Therefore, it can be concluded that the LDH nanosheets adsorbed alginate chains on two surfaces (Costantino, Coletti, Nocchetti, Aloisi, & Elisei, 1999; Williams, Norquist, & O'Hare, 2004).

Through different drying methods, we can obtain many layered alginate/LDH nanocomposites, as shown in Fig. 4a–d. Clearly, the typical LDH diffraction peak of (1 1 0) reflection at $2\theta = 61^\circ$ can be observed on the XRD curves of the resultant nanocomposites (Fig. 4a–d). The pattern contains a set of basal reflections (0 0 l), confirming the layered structure. The broad diffraction peaks suggest that the interlayer distances are not uniform. The basal spacing varies from 0.82 to 0.67 nm (Fig. 4a–d) and is independent of the drying methods. Taking into account the thickness of the LDH layer (about 0.48 nm (Khan & O'Hare, 2002)), the increase of the interlayer distance (Δd) in the alginate/LDH nanocomposite is about 0.19–0.34 nm. Given that the LDH nanosheets adsorbed the alginate chains, the alginate chains envelop the nanosheet into a sandwich-like layered structure, a bilayer arrangement of the alginate molecules should be formed in the interlayer of the dried nanocomposites after evaporating water (Costantino et al., 1999; Iyi, Kurashima, & Fujita, 2002). Alginate/LDH composites, prepared by coprecipitation, have been reported to have d-spacings of 1.304 and 1.320 nm with interlayer distances of 0.82–0.84 nm; these spacings indicate the alginate units were arranged in a stretched monolayer in the interlayer of LDH (Darder et al., 2005; Leroux et al., 2004). In the present work, the alginate units occupy double layers with an interlayer distance of 0.19–0.34 nm, suggesting that the alginate molecules are in a more confined state. In the TEM image a layered structure in alginate/LDH nanocomposite can be clearly observed (Fig. 5A), agreeing with the XRD result.

On the FTIR spectrum of the dried alginate/LDH nanocomposite, the characteristic absorbance band of metal–oxygen bonds in LDH layers is clearly shown at 446 cm^{-1} (Fig. 3d). The absorbance bands of the antisymmetric and symmetric stretching vibrations of —COO^- at 1615 and 1417 cm^{-1} for alginate (Fig. 3c) shift to lower wavenumbers of 1609 and 1411 cm^{-1} (Fig. 3d), respectively. The shift of the absorbance bands of —COO^- indicates the interaction between the carboxyl groups of alginate and LDH. Similar results have been found during the intercalation of alginate into LDH (Darder et al., 2005).

An alginate/LDH nanocomposite, prepared from a ratio of aqueous alginate:LDH in formamide of 0.8:1, and referred to as alginate/LDH nanocomposite-I (Table 1), was re-dispersed in water. The LDH nanosheets were stabilized by the alginate adsorbed to the sheets. The LDH nanosheets with the adsorbed alginate were then concentrated by centrifugation and the resultant alginate/LDH colloidal suspension remained in an amorphous state, showing no signs of LDH aggregation (Fig. 4e). In previous work, carboxymethyl cellulose was also found to have a stabilizing effect on LDH (Kang et al., 2009). Considering the similarity of alginate and carboxymethyl cellulose, it should be expected that other polysaccharide derivatives, with the similar structures and charges, could also have a stabilizing effect on LDH nanosheets.

TGA curves of pure alginate, NO_3^-–LDH, and the alginate/LDH nanocomposite-I are shown in Fig. 6. For pure alginate (Fig. 6a), the observed weight loss of 8% below 200 °C is attributed to the evaporation of physically adsorbed water. From 200 °C to 586 °C, the weight loss of 52% is attributed to thermal degradation and combustion, and beyond 586 °C weight loss may be attributed to the decomposition of resultant sodium salts. However, for the NO_3^-–LDH (Fig. 6b), the observed weight loss of about 8% due to water evaporation is observed in the temperature range 20–174 °C. About 40% weight loss is observed between 174 °C and 568 °C which is due to the removal of the NO_3^- anions in the interlayer and the dehydroxylation of the layers. Fig. 6c represents the thermogravimetric curve for the alginate/LDH nanocomposite-I. The observed weight loss of about 13% between 20 °C and 195 °C is related to

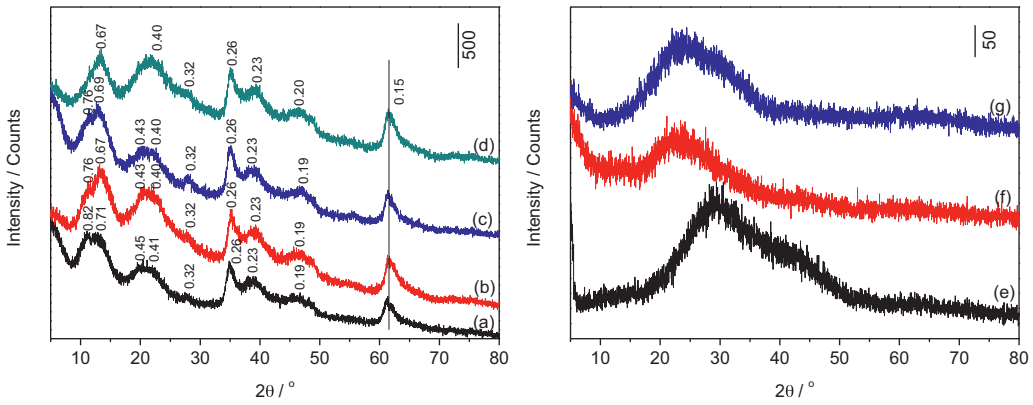

Fig. 4. XRD patterns of alginate/LDH nanocomposites by (a) and (c) freeze-dried and (b) and (d) dried *in vacuo* at 30 °C (volume ratios of alginate solution and LDH nanosheets solution with 0.8/1 (a) and (b) and 0.6/1 (c) and (d) (V/V)), (e) dried alginate/LDH nanocomposite after being re-dispersed in water, and the membranes of alginate/LDH nanocomposite prepared by mixing different volume ratios of alginate solution and LDH nanosheets solution where the volume ratio for (f) is 0.6/1 and for (g) is 0.8/1 (V/V). *d* in nanometer.

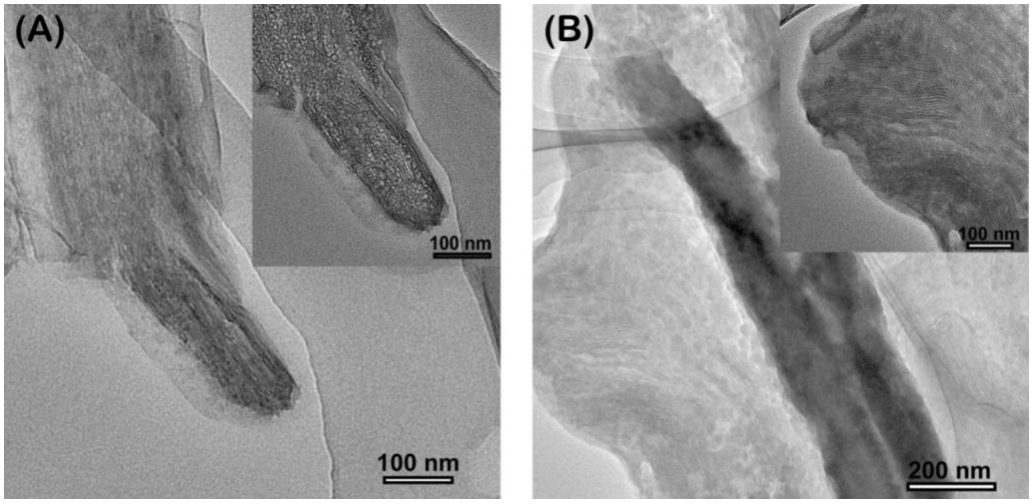

Fig. 5. TEM photos of (A) alginate/LDH nanocomposite and (B) alginate/LDH nanocomposite membrane.

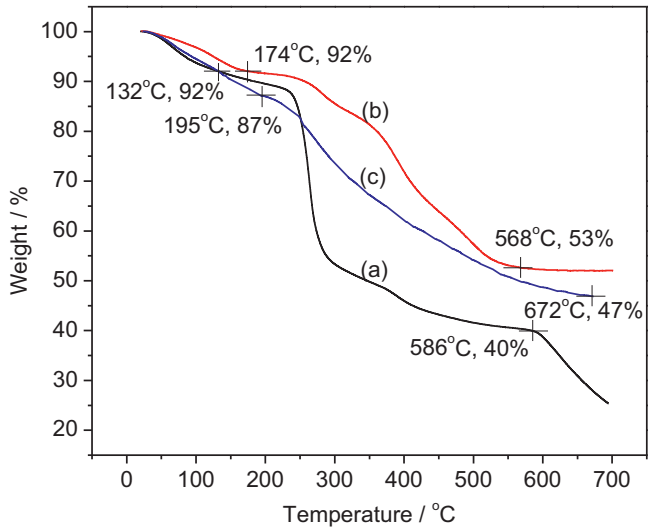

Fig. 6. TGA curves of (a) alginate, (b) NO_3^-–LDH and (c) alginate/LDH nanocomposite (alginate/LDH nanocomposite-I).

the loss of water. In the temperature range 195–672 °C, the weight loss (40%) is attributed to the dehydroxylation of the LDH layers as well as to the degradation and combustion of alginate. Upon comparing the thermogravimetry of alginate (Fig. 6a) and alginate/LDH nanocomposite-I (Fig. 6c), it can be seen that the thermal stability of alginate in the nanocomposite has increased.

Alginate/LDH nanocomposite membranes were prepared, as mentioned earlier, by dialyzing the mixture of aqueous alginate and LDH in formamide against water to remove the formamide, and then evaporating the water. Two membranes were prepared, one (alginate/LDH nanocomposite membrane-I) with LDH content of 20 wt.%, and the second (alginate/LDH nanocomposite membrane-II) with LDH content of 15.8 wt.%. These membranes were found to contain 80 and 84.2 wt.% alginate which is significantly more alginate than was found in the original preparation of an alginate/LDH nanocomposites (37 wt.%). The powder XRD patterns for both of these nanocomposite membranes are typical amorphous diffraction patterns in the range 16°–38° (Fig. 4g and f). However, TEM images (Fig. 5B) show isolated areas containing layered structures in the membranes. Perhaps, the small numbers of these assemblies of LDH/alginate nanosheets are swamped by the bulk alginate matrix. The mechanical properties of the

Table 2
Mechanical properties of alginate and alginate/LDH nanocomposite membranes.

Samples	Content of LDH (wt.%)	Young's modulus (MPa)	Tensile strength at break (MPa)	Tensile elongation at break (%)
Alginate membrane	0	2426 ± 178	28 ± 4	2 ± 0.4
Alginate/LDH membrane-I	15.8	3047 ± 275	46 ± 2	2 ± 0.6
Alginate/LDH membrane-II	20	5331 ± 46	68 ± 5	4.2 ± 1.0

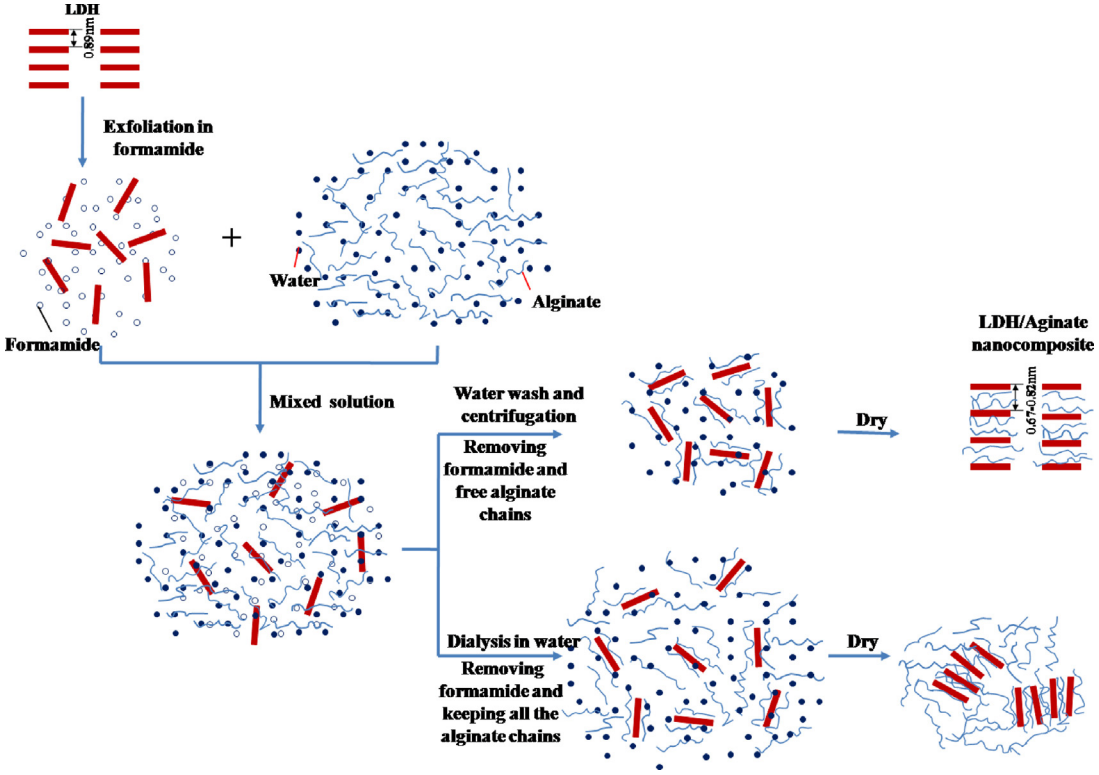

Scheme 2. A schematic of the control process for converting LDH nanosheets dispersions into alginate/LDH nanocomposites.

alginate/LDH nanocomposite membrane and alginate membrane were evaluated; the results are listed in Table 2. At an LDH content of up to 20 wt.% the nanocomposite membrane remains in a homogeneously dispersed state. The addition of LDH into the alginate matrix leads to an increase in the Young's modulus, tensile strength at break and tensile elongation at break.

3.4. The formation of the structure of LDH nanosheets in an alginate matrix

The structure formation of LDH nanosheets in an alginate matrix is shown in Scheme 2. LDH nanosheet surfaces are coated on both sides with alginate when those nanosheets are dispersed in formamide and mixed with aqueous alginate solution. This arises through electrostatic interactions that form between the positive and negative charges of the alginate chains and the LDH surface. The alginate coating prevents restacking of LDH nanosheets after removal of the formamide. Therefore, the LDH nanosheets coated by the alginate chains are kinetically stable in water. When both the formamide solvent and the free alginate chains are removed by water washing and centrifugation, the colloidal nanosheets with adsorbed alginate chains flocculate and restack into layered nanocomposites after the water has been evaporated. Moreover, when excess alginate molecules remain in solution, as is the case of a dialyzed alginate/formamide mixture which removes only formamide leaving free alginate molecules in solution in addition to those adsorbed onto LDH nanosheets, only localized restacking of alginate-LDH nanosheets can occur within the alginate matrix.

4. Conclusions

NO_3^-–LDH was exfoliated in formamide into nanosheets with positive charges. These positively charged nanosheets could be stabilized in an aqueous solution through complexation with alginate molecules that possess negative charges. Here, alginate chains were adsorbed on the LDH nanosheets to form a "sandwich" structure by static interaction. When formamide and free alginate in the mixed solution of LDH and alginate were removed by water washing and ultracentrifugation, a colloidal alginate/LDH mixture was obtained. After evaporating water from the sample, the colloid restacked into a layered structure nanocomposite with intercalcation of alginate chains in the interlayers of LDH, having the basal spacing from 0.82 to 0.67 nm. In contrast, if a significant quantity of free alginate chains remained in solution, in excess of those adsorbed onto LDH nanosheets, after drying the alginate/LDH nanocomposite into a membrane the membrane contained localized areas of stacked alginate/LDH nanosheets dispersed within the alginate matrix. After the alginate/LDH nanocomposites were redissolved in water, the LDH nanosheets could be re-dispersed and stabilized by the absorbed alginate in water. The thermal stability of alginate in a nanocomposite was increased by LDH. The addition of LDH into the alginate matrix led to an increase in mechanical properties.

Acknowledgements

The financial support provided by the National Natural Science Foundation for younger scientists of China (Grant No. 51003108) to carry out this work is greatly appreciated. The helpful discussions and language corrections from Dr. Sheila M. Murphy are greatly appreciated.

References

Adachi-Pagano, M., Forano, C., & Besse, J. P. (2000). Delamination of layered double hydroxides by use of surfactants. *Chemical Communications*, (1), 91–92.

Alcantara, A. C. S., Aranda, P., Darder, M., & Ruiz-Hitzky, E. (2010). Bionanocomposites based on alginate-zein/layered double hydroxide materials as drug delivery systems. *Journal of Materials Chemistry*, *20*(42), 9495–9504.

Ayari, A., Cobas, E., Ogundadegbe, O., & Fuhrer, M. S. (2007). Realization and electrical characterization of ultrathin crystals of layered transition-metal dichalcogenides. *Journal of Applied Physics*, *101*(1), 014507.

Costantino, U., Coletti, N., Nocchetti, M., Aloisi, G. G., & Elisei, F. (1999). Anion exchange of methyl orange into Zn-Al synthetic hydrotalcite and photophysical characterization of the intercalates obtained. *Langmuir*, *15*(13), 4454–4460.

Darder, M., Lopez-Blanco, M., Aranda, P., Leroux, F., & Ruiz-Hitzky, E. (2005). Bionanocomposites based on layered double hydroxides. *Chemistry of Materials*, *17*(8), 1969–1977.

Fabia, J., Slusarczyk, C., Gawlowski, A., Graczyk, T., Wlochowicz, A., & Janicki, J. (2005). Supermolecular structure of alginate fibres for medical applications studied by means of WAXS and SAXS methods. *Fibres & Textiles in Eastern Europe*, *13*(5), 114–117.

Gordon, R. A., Yang, D., Crozier, E. D., Jiang, D. T., & Frindt, R. F. (2002). Structures of exfoliated single layers of WS2, MoS2, and MoSe2 in aqueous suspension. *Physical Review B*, *65*(12), 125–407.

Hibino, T. (2004). Delamination of layered double hydroxides containing amino acids. *Chemistry of Materials*, *16*(25), 5482–5488.

Hibino, T., & Jones, W. (2001). New approach to the delamination of layered double hydroxides. *Journal of Materials Chemistry*, *11*(5), 1321–1323.

Hibino, T., & Kobayashi, M. (2005). Delamination of layered double hydroxides in water. *Journal of Materials Chemistry*, *15*(6), 653–656.

Hong, B. J., Compton, O. C., An, Z., Eryazici, I., & Nguyen, S. T. (2012). Successful stabilization of graphene oxide in electrolyte solutions: Enhancement of biofunctionalization and cellular uptake. *ACS Nano*, *6*(1), 63–73.

Ida, S., Ogata, C., Eguchi, M., Youngblood, W. J., Mallouk, T. E., & Matsumoto, Y. (2008). Photoluminescence of perovskite nanosheets prepared by exfoliation of layered oxides, K(2)Ln(2)Ti(3)O(10), KLnNb(2)O(7), and RbLnTa(2)O(7) (Ln: lanthanide ion). *Journal of the American Chemical Society*, *130*(22), 7052–7059.

Ida, S., Shiga, D., Koinuma, M., & Matsumoto, Y. (2008). Synthesis of hexagonal nickel hydroxide nanosheets by exfoliation of layered nickel hydroxide intercalated with dodecyl sulfate ions. *Journal of the American Chemical Society*, *130*(43), 14038–14039.

Iyi, N., Kurashima, K., & Fujita, T. (2002). Orientation of an organic anion and second-staging structure in layered double-hydroxide intercalates. *Chemistry of Materials*, *14*(2), 583–589.

Iyi, N., Okamoto, K., Kaneko, Y., & Matsumoto, T. (2005). Effects of anion species on deintercalation of carbonate ions from hydrotalcite-like compounds. *Chemistry Letters*, *34*(7), 932–933.

Jiao, C. M., Chen, X. L., & Zhang, J. (2010). Synergistic flame-retardant effects of aluminum oxide with layered double hydroxides in EVA/LDH composites. *Journal of Thermoplastic Composite Materials*, *23*(4), 501–512.

Kang, H. L., Huang, G. L., Ma, S. L., Bai, Y. X., Ma, H., Li, Y. L., et al. (2009). Coassembly of Inorganic Macromolecule of Exfoliated LDH Nanosheets with Cellulose. *Journal of Physical Chemistry C*, *113*(21), 9157–9163.

Khan, A. I., & O'Hare, D. (2002). Intercalation chemistry of layered double hydroxides: Recent developments and applications. *Journal of Materials Chemistry*, *12*(11), 3191–3198.

Kim, T. W., Oh, E. J., Jee, A. Y., Lim, S. T., Park, D. H., Lee, M., et al. (2009). Soft-chemical exfoliation route to layered cobalt oxide monolayers and its application for film deposition and nanoparticle synthesis. *Chemistry – A European Journal*, *15*(41), 10752–10761.

Knieke, C., Berger, A., Voigt, M., Taylor, R. N. K., Rohrl, J., & Peukert, W. (2010). Scalable production of graphene sheets by mechanical delamination. *Carbon*, *48*(11), 3196–3204.

Kuila, T., Khanra, P., Bose, S., Kim, N. H., Ku, B. C., Moon, B., et al. (2011). Preparation of water-dispersible graphene by facile surface modification of graphite oxide. *Nanotechnology*, *22*(30), 305710.

Lee, S. Y., & Kim, S. J. (2002). Delamination behavior of silicate layers by adsorption of cationic surfactants. *Journal of Colloid and Interface Science*, *248*(2), 231–238.

Leroux, F., Gachon, J., & Besse, J. P. (2004). Biopolymer immobilization during the crystalline growth of layered double hydroxide. *Journal of Solid State Chemistry*, *177*(1), 245–250.

Li, J. M. (2010). Mass production of graphene-like single-crystalline $NbSe_2$ (004) nanosheets via intercalant-assisted thermal cleavage. *Applied Physics A – Materials Science & Processing*, *99*(1), 229–235.

Li, L., Ma, R. Z., Ebina, Y., Iyi, N., & Sasaki, T. (2005). Positively charged nanosheets derived via total delamination of layered double hydroxides. *Chemistry of Materials*, *17*(17), 4386–4391.

Liu, Z., Robinson, J. T., Sun, X. M., & Dai, H. J. (2008). PEGylated nanographene oxide for delivery of water-insoluble cancer drugs. *Journal of the American Chemical Society*, *130*(33), 10876–10877.

Liu, Z. P., Ma, R. Z., Osada, M., Iyi, N., Ebina, Y., Takada, K., et al. (2006). Synthesis, anion exchange, and delamination of Co-Al layered double hydroxide: Assembly of the exfoliated nanosheet/polyanion composite films and magneto-optical studies. *Journal of the American Chemical Society*, *128*(14), 4872–4880.

Ma, X. Y., Chai, Y. Y., Evans, D. G., Li, D. Q., & Feng, J. T. (2011). Preparation and selective acetylene hydrogenation catalytic properties of supported Pd catalyst by the in situ precipitation-reduction method. *Journal of Physical Chemistry C*, *115*(17), 8693–8701.

Manohara, G. V., Prasanna, S. V., & Kamath, P. V. (2011). Structure and composition of the layered double hydroxides of Mg and Fe: Implications for anion-exchange reactions. *European Journal of Inorganic Chemistry*, (16), 2624–2630.

Mas-Balleste, R., Gomez-Navarro, C., Gomez-Herrero, J., & Zamora, F. (2011). 2D materials: To graphene and beyond. *Nanoscale*, *3*(1), 20–30.

Masuda, Y., Hamada, Y., Seo, W. S., & Koumoto, K. (2006). Exfoliation of layers in NaxCoO2. *Journal of Nanoscience and Nanotechnology*, *6*(6), 1632–1638.

Nethravathi, C., & Rajamathi, M. (2008). Chemically modified graphene sheets produced by the solvothermal reduction of colloidal dispersions of graphite oxide. *Carbon*, *46*(14), 1994–1998.

Novoselov, K. S., Geim, A. K., Morozov, S. V., Jiang, D., Zhang, Y., Dubonos, S. V., et al. (2004). Electric field effect in atomically thin carbon films. *Science*, *306*(5696), 666–669.

Novoselov, K. S., Jiang, D., Schedin, F., Booth, T. J., Khotkevich, V. V., Morozov, S. V., et al. (2005). Two-dimensional atomic crystals. *Proceedings of the National Academy of Sciences of the United States of America*, *102*(30), 10451–10453.

Ogawa, M., & Kaiho, H. (2002). Homogeneous precipitation of uniform hydrotalcite particles. *Langmuir*, *18*(11), 4240–4242.

Omomo, Y., Sasaki, T., Wang, L. Z., & Watanabe, M. (2003). Redoxable nanosheet crystallites of MnO_2 derived via delamination of a layered manganese oxide. *Journal of the American Chemical Society*, *125*(12), 3568–3575.

Osada, M., Ebina, Y., Takada, K., & Sasaki, T. (2006). Gigantic magneto-optical effects in multilayer assemblies of two-dimensional titania nanosheets. *Advanced Materials*, *18*(3), 295–299.

Osada, M., & Sasaki, T. (2009). Exfoliated oxide nanosheets: New solution to nanoelectronics. *Journal of Materials Chemistry*, *19*(17), 2503–2511.

Parvulescu, A. N., Hausoul, P. J. C., Bruijnincx, P. C. A., Korhonen, S. T., Teodorescu, C., Gebbink, R., et al. (2011). Telomerization of 1,3-butadiene with biomass-derived alcohols over a heterogeneous Pd/TPPTS catalyst based on layered double hydroxides. *ACS Catalysis*, *1*(5), 526–536.

Rabu, P., & Drillon, M. (2003). Layered organic–inorganic materials: A way towards controllable magnetism. *Advanced Engineering Materials*, *5*(4), 189–210.

Ray, S. S., & Okamoto, M. (2003). Polymer/layered silicate nanocomposites: A review from preparation to processing. *Progress in Polymer Science*, *28*(11), 1539–1641.

Sakamoto, J., van Heijst, J., Lukin, O., & Schluter, A. D. (2009). Two-dimensional polymers: Just a dream of synthetic chemists? *Angewandte Chemie-International Edition*, *48*(6), 1030–1069.

Sakugawa, K., Ikeda, A., Takemura, A., & Ono, H. (2004). Simplified method for estimation of composition of alginates by FTIR. *Journal of Applied Polymer Science*, *93*(3), 1372–1377.

Sasaki, T., & Watanabe, M. (1998). Osmotic swelling to exfoliation. Exceptionally high degrees of hydration of a layered titanate. *Journal of the American Chemical Society*, *120*(19), 4682–4689.

Takei, T., Yonesaki, Y., Kumada, N., & Kinomura, N. (2008). Preparation of oriented titanium phosphate and tin phosphate/polyaniline hybrid films by electrochemical deposition. *Langmuir*, *24*(16), 8554–8560.

Tanaka, T., Ebina, Y., Takada, K., Kurashima, K., & Sasaki, T. (2003). Oversized titania nanosheet crystallites derived from flux-grown layered titanate single crystals. *Chemistry of Materials*, *15*(18), 3564–3568.

Wang, D. Y., Das, A., Costa, F. R., Leuteritz, A., Wang, Y. Z., Wagenknecht, U., et al. (2010). Synthesis of organo cobalt aluminum layered double hydroxide via a novel single-step self-assembling method and its use as flame retardant nanofiller in PP. *Langmuir*, *26*(17), 14162–14169.

Widenkvist, E., Boukhvalov, D. W., Rubino, S., Akhtar, S., Lu, J., Quinlan, R. A., et al. (2009). Mild sonochemical exfoliation of bromine-intercalated graphite: A new route towards graphene. *Journal of Physics D – Applied Physics*, *42*(11), 112003–112007.

Williams, G. R., Norquist, A. J., & O'Hare, D. (2004). Time-resolved, in situ X-ray diffraction studies of staging during phosphonic acid intercalation into LiAl2OH)(6) Cl center dot H2O. *Chemistry of Materials*, *16*(6), 975–981.

Xiao, H., Chen, X., Ji, L. Y., Zhang, X., & Yang, W. S. (2007). Direct electrochemistry of myoglobin in MnO_2 nanosheet film. *Chemistry Letters*, *36*(6), 772–773.

Zhang, J. P., Wang, Q., Xie, X. L., Li, X., & Wang, A. Q. (2010). Preparation and swelling properties of pH-sensitive sodium alginate/layered double hydroxides hybrid beads for controlled release of diclofenac sodium. *Journal of Biomedical Materials Research Part B – Applied Biomaterials*, *92B*(1), 205–214.